MULTISPECTRAL QUICKBIRD-2 IMAGE SEGMENTATION BASED ON VECTOR FIELD MODEL

P. Xiao

Department of Geographical Information Science, Nanjing University, Nanjing 210093, P. R. China - xiaopf@gmail.com

WgS-PS: WG IV/9 - Mapping from High Resolution Data

KEY WORDS: Land Cover, Segmentation, Image Processing, Automation, Feature Extraction, Quickbird

ABSTRACT:

Image segmentation is a valuable approach that performs an object-based rather than a pixel-based analysis of high-spatial resolution satellite image. A multiscale approach for segmenting the pan-sharpened multispectral QuickBird-2 image based on vector field model is proposed. The edge features are obtained using the first fundamental form of the multispectral bands. The response of log Gabor bank filtering of each band is fused as multiscale texture features based on first fundamental form. Then, the image segmentation is implemented based on texture-marked watershed transform. The segmentation accuracy is assessed using discrepancy measures between a reference map and the segmentation. The experimental results show that the proposed approach gives a better solution of integrating spectral and texture information for the segmentation of multispectral remotely sensed image.

1. INTRODUCTION

While remote sensing has made enormous progress over recent years and a variety of sensors, such as IKONOS-2, QuickBird-2, OrbView-4, deliver high resolution data on an operational basis, a vast majority of applications still rely on basic image processing concepts developed in the early 1970s: classification of single pixels in a multi-dimensional feature space. In most cases, information important for the understanding of an image is not represented in single pixels but in meaningful image objects. Procedures for image segmentation which are able to dissect images into sets of useful image objects are therefore a prerequisite for the successful automation of image interpretation (Blaschke *et al*, 2000).

Despite some early research activities (Kettig and Landgrebe, 1976), image segmentation was established relatively late in the field of remote sensing (e.g. Ryherd and Woodcock, 1996), and has rarely featured thus far in image processing (Schiewe, 2002). Although there has been a lot of development in the segmentation of remotely sensed image (e.g. Pal *et al*., 2000; Pesaresi and Benediktsson, 2001; Pekkarinen, 2002; Acharyya *et al*., 2003; Devereuxa *et al*., 2004; Li and Gong, 2005; Hu *et al*., 2005; Chen *et al*., 2006; Lia *et al*., 2007; Wang and Boesch *et al*., 2007), there has been little progress in the segmentation of multispectral image (e.g. Kartikeyan *et al*., 1998; Baatz and Schape, 1999; Evans *et al*., 2002; Sarkar *et al*., 2002; Li and Xiao, 2007).

Remote sensing sensors are producing multispectral so that in contrast to the most often used greyscale image in the disciplines not only the complexity but also the redundancy increases. Early approaches to considering multispectral image attempted to combine the response of each bands. The way are combined is, in general, heuristic, and has no theoretical basis (Sapiro and Ringbach, 1996). A principled way to look at multispectral image is vector field model (Zenzo, 1986; Cumani, 1991). The value of multispectral image at a given point can be regarded as N-dimensional vector in $\mathbf{R}^N$, and the difference of image values can be defined from the theory of surfaces in differential geometry. In the research, method of first funda-mental form (Sapiro and Ringbach, 1996; Scheunders, 2002) is applied to the definition of gradient and fusion of texture from multispectral remotely sensed image.

Watershed transform is a powerful morphological tool for image segmentation that is usually defined for greyscale image (Vincent and Soille, 1991). This paper presents an extension of the watershed algorithm for multispectral image segmentation. As shown in Figure 1, edge features are obtained using the first fundamental form of multispectral bands. For solving the over-segmentation problem of watershed transform, The response of log Gabor bank filtering of each band is fused as multiscale texture features also based on first fundamental form. Then the image segmentation is implemented based on texture-marked watershed transform. Finally, The segmentation accuracy is assessed using discrepancy measures between a reference map and the segmentation.

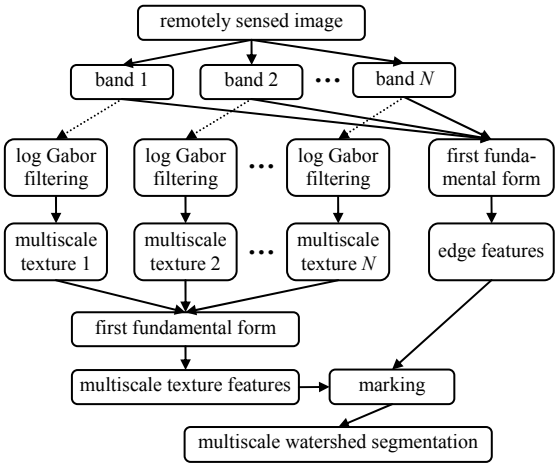

Figure 1. The scheme for multispectral image segmentation

2. METHOD

2.1 First Fundamental Form

The vector-field way to look at gradient in multispectral image has been described from Zenzo (1986) to Scheunders (2002). The idea is the following. Let $\mathbf{I}(x, y)$: $\mathbf{R}^2 \rightarrow \mathbf{R}^N$ be a multispectral image with bands $\mathbf{I}_i(x, y)$: $\mathbf{R}^2 \rightarrow \mathbf{R}$, $i = 1, ..., N$. The value of $\mathbf{I}$ at a given point (x_0, y_0) is a N-dimensional vector in $\mathbf{R}^N$, then the multispectral image can be seen as a vector field. The difference of image values at two points $P = (x_0, y_0)$ and $Q = (x_1, y_1)$ is given by

$$\Delta\mathbf{I} = \mathbf{I}(P) - \mathbf{I}(Q). \tag{1}$$

When the Euclidean distance $d(P, Q)$ between P and Q tends to zero, the difference becomes the arc element

$$d\mathbf{I} = \frac{\partial \mathbf{I}}{\partial x}dx + \frac{\partial \mathbf{I}}{\partial y}dy \tag{2}$$

and its squared norm is given by

$$d\mathbf{I}^2 = \begin{pmatrix} dx \\ dy \end{pmatrix}^T \begin{pmatrix} \left(\frac{\partial \mathbf{I}}{\partial x}\right)^2 & \frac{\partial \mathbf{I}}{\partial x}\frac{\partial \mathbf{I}}{\partial y} \\ \frac{\partial \mathbf{I}}{\partial y}\frac{\partial \mathbf{I}}{\partial x} & \left(\frac{\partial \mathbf{I}}{\partial y}\right)^2 \end{pmatrix} \begin{pmatrix} dx \\ dy \end{pmatrix} = \begin{pmatrix} dx \\ dy \end{pmatrix}^T \begin{pmatrix} G_{xx} & G_{xy} \\ G_{yx} & G_{yy} \end{pmatrix} \begin{pmatrix} dx \\ dy \end{pmatrix}. \tag{3}$$

This quadratic form is called the first fundamental form. It allows the measurement of changes in a multispectral image. The extreme of the quadratic form (3) are obtained in the directions of the eigenvectors of the 2×2 matrix

$$\mathbf{G} = \begin{pmatrix} G_{xx} & G_{xy} \\ G_{yx} & G_{yy} \end{pmatrix} \tag{4}$$

and the values attained there are the corresponding eigenvalues. Simple algebra shows that the eigenvalues are

$$\lambda_{\pm} = \frac{G_{xx} + G_{yy} \pm \sqrt{(G_{xx} - G_{yy})^2 + 4G_{xy}^2}}{2} \tag{5}$$

and the eigenvectors are $(\cos\theta_{\pm}, \sin\theta_{\pm})$, where the angles $\theta_{\pm}$ are given by

$$\theta_{+} = \frac{1}{2}\arctan\frac{2G_{xy}}{G_{xx} - G_{yy}},$$
$$\theta_{-} = \theta_{+} + \frac{\pi}{2}. \tag{6}$$

Thus, the eigenvectors provide the direction of maximal and minimal changes at a given point in the multispectral image, and the eigenvalues are the corresponding rates of change.

The multispectral discontinuities can be detected by defining a function $f = f(\lambda_+, \lambda_-)$ that measures the dissimilarity between λ_+ and λ_-. A possible choice, the one adopted in the research, is

$$f = \sqrt{\lambda_+ - \lambda_-} \tag{7}$$

which has the nice property of reducing to $d\mathbf{I}^2$ for the one-dimensional case.

For multispectral image, a single-valued approach can be adopted by segmenting each band separately, or by first combining the bands into a single grey image. The concept of the first fundamental form however allows to access gradient information from all bands simultaneously (Scheunders, 2002). Furthermore, the first fundamental form can be used in image fusion (e.g. Scheunders, 2001). So it is implemented in the research to fuse the texture features of all bands.

2.2 Log Gabor Bank Filtering

For solving the over-segmentation problem of watershed transform, texture features are considered to mark edge features. In order to produce texture features, it is need to characterise the texture content of the image at each pixel. One of the most popular techniques is the use of a bank of differently scaled and orientated complex Gabor filters (Jain and Farrokhnia, 1991). Gabor filter has the capability of reaching the minimum bound for simultaneous localization in the space and frequency domains. However, the Gabor filter is mathematically pure in only the Cartesian coordinates where all the Gabor channels are the same size in frequency and hence have sensors that are all the same size in space. An objective of the filter design might be to obtain as broad as possible spectral information with maximal spatial localization in the research. One cannot construct Gabor function of arbitrarily wide bandwidth and still maintain a reasonably small Direct Centre (DC) component in the even-symmetric filter (Kovesi, 1996).

Based on the characteristics of annular-distribution of Fourier spectrum in logarithmic coordinates, an alternative to the Gabor function is the log Gabor function proposed first by Field (1987). On the linear frequency scale the log Gabor function has a transfer function of the form

$$G(f) = \exp\left\{\frac{-[\log(f / f_0)]^2}{2[\log(\sigma / f_0)]^2}\right\} \tag{8}$$

where f_0 is the filter's centre frequency. To obtain constant shape ratio filters the term σ/f_0 must also be held constant for varying f_0. There are two important characters for log Gabor function. Firstly, log Gabor function, by definition, always has no DC component, and secondly, the transfer function of the log Gabor function has an extended tail at the high frequency end, which conquers the over-representation in low frequency components (Kovesi, 1996).

The filter is constructed directly in the frequency domain as polar-separable functions: a logarithmic Gaussian function in the radial direction and a Gaussian in the angular direction. The ratio between the angular spacing of the filters and angular standard deviation of the Gaussians is 1.2. A log Gabor filter bank comprising filters with different parameters of log Gabor functions provides a complete cover of spatial frequency domain so that it can generate a versatile model for texture description.

Applying the complex-valued log Gabor filter to remotely sensed imagery $I(x, y)$ yields a complex response $R(x, y)$ with respective real and imaginary components

$$R(x, y) = R_r(x, y) + jR_i(x, y). \tag{9}$$

The response $R(x, y)$ can be computed either by calculating $R_r(x, y)$ and $R_i(x, y)$ separately by 2-D convolution or directly

via Fourier transform inversion. Because image $R(x, y)$ is an analytic signal, $R_r(x, y)$ and $R_i(x, y)$ form a quadrature pair. The amplitude envelopes of $R(x, y)$ may be recovered via

$$A(x, y) = \sqrt{R_r^2(x, y) + R_i^2(x, y)} \quad (10)$$

The amplitude response $A(x, y)$ is regarded as the texture features in the research.

The log Gabor filter bank is used to convolute with each band to derive texture response in each scale and orientation. Combining the texture information in all orientations, multi-scale texture features of each band are obtained.

2.3 Watershed Transform

The watershed transform is a well-known powerful tool for automated image segmentation. Because its resulting boundaries form closed and connected regions, it becomes one of the best choices of the segmentation of remotely sensed image (e.g. Li *et al*., 1999; Hall *et al*., 2004; Chen *et al*., 2006; Li and Xiao, 2007), which need recognise all of the objects in the image. The presented watershed algorithm is based on an immersion process analogy (Vincent and Soille, 1991), in which the flooding of the water in the image is efficiently simulated using a queue of pixels.

Watershed transform often produce over-segmentation in situations of high gradient noise, quantity error and detailed texture. There are many solutions to the problem. A marker based solution is chosen in this research that basins are flooded from selected sources rather than minima. To integrate the edge and texture information of the landscape objects in image, watershed transform is implemented based on edge features, and the marker image is calculated from texture features. The texture features are segmented at first using a moving threshold algorithm developed from Hill *et al*. (2003). This algorithm calculates the mean and standard deviation of the texture features. Then several binary images are produced at reasonably spaced thresholds using the mean and standard deviation. For each binary image, the number of closed and connected regions greater than the given minimum size is calculated. The threshold with the maximum number of connected regions is used as the output marker image. With this algorithm, no a priori knowledge is required about the number of regions. One only needs to give the size of the minimum region, which is always constant to most images.

The edge features can be reconstructed with the marker image and then be segmented based on the watershed transform. The image has produced several scale texture features after the log Gabor bank filtering. Use different frequency of the texture features can produce segmentation results in different scale. Generally, low-frequency texture features produce large-scale segmentation results, whereas high-frequency texture features produce small-scale segmentation results.

2.4 Accuracy Assessment

The decision of the best segmentation results usually relies on the accuracy assessment. However, similar to the segmentation theory there is no established procedure for the assessment of its results. A general classification of assessment methods has been proposed by Zhang (1996), but only very few studies employ the assessment on remotely sensed image. Carleer *et al.* (2005) proposed a supervised method using discrepancy measures between a reference and the segmentation, which is employed in the research.

The reference map is obtained interpreting from the original image by remote sensing experts. The reference polygons then are converted to raster. To compare the discrepancy, the segmentation results are overlaid on the reference map. Observing from each segment region, the largest part in the reference map is regarded as right segmentation of this region, the others are regarded as mix-segmented pixels. Two discrepancy evaluations are calculated: percentage of Right-Segmented pixels in the whole image (*RS*), and ratio of Region Count in segmented image to reference map (*RC*). For an excellent segmentation, *RS* will be close to 100%, and *RC* will equal to 1. In the assessment method based on reference map, if only *RS* is used, *RS* will be increased with the fragmentation of the segmentation, even it will be equal to 100% when the region size equal to one pixel, which becomes a meaningless segmentation. So *RC* is also important indicator to restrict the segment regions close to the reference regions.

3. DATA

The data used throughout the research is a 512×512 pixel subimage of a QuickBird-2 scene acquired in November 21, 2004 (Figure 2). Geographically, this area represents a portion of the highly fragmented agricultural landscape typical of the Jiangning region of Nanjing, China. QuickBird-2 provides 16bit multispectral data in the red, green, blue and near-infrared bands at 2.4m spatial resolution and an 11bit panchromatic band at 0.6m resolution. For producing high-resolution multispectral images, the multispectral bands are sharpened to 0.6m resolution using panchromatic band based on Pansharp method proposed by Zhang (2002) at first. The false colour image for shown in Figure 2 is composed with infrared, red, and green band. In the false colour image, the red colour represents vegetation, the black colour indicates water, and the white colour represents roads.

Figure 2. Original image overlaid reference polygons

4. RESULTS

The edge features are computed based on the first fundamental form of the multispectral bands. It is shown in Figure 3 that the edge detection results are uninterrupted, and important edges have been preserved, but there is much noise in the texture region. So the texture marking is required to segmentation.

The multiscale texture features of each band are calculated from the response of log Gabor bank filtering. Each band is filtered separately using 2 octave bandwidth log Gabor filter bank over 6 orientations and 4 frequencies. The wavelength of the highest frequency filters is 3 pixels. The scaling between successive filters is 2. Thus, 4 scale texture features are produced for each band. Then, the texture features of all bands are fused in scales based on first fundamental form.

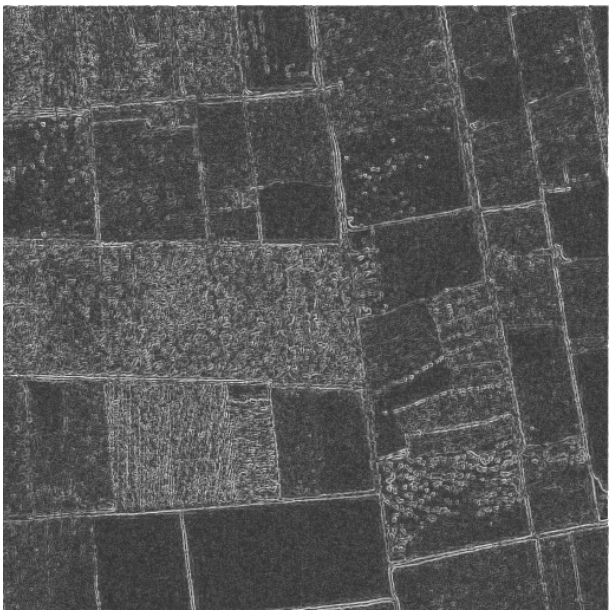

Figure 3. Edge features of multispectral bands

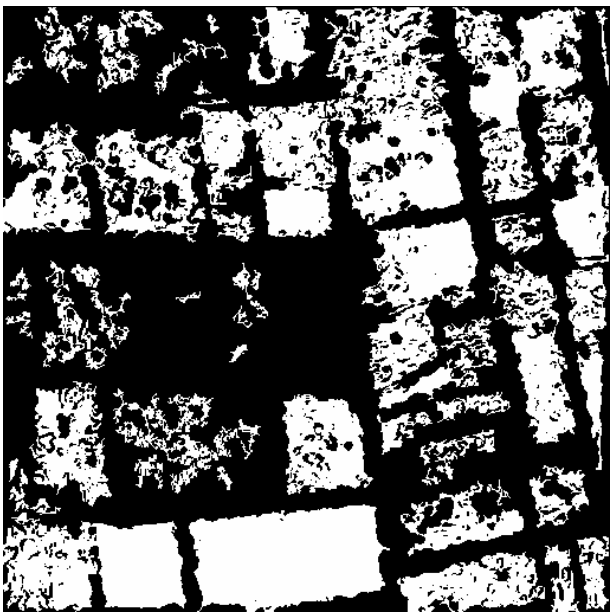

Figure 4. Texture marker in scale 2

For obtaining marker image for watershed segmentation, the texture features are segmented using the moving threshold algorithm, in which 50 pixels is used as the minimum region size. Figure 4 shows the texture marker in scale 2, in which the texture regions are marked distinctly.

Then, edge features are segmented based on texture-marked watershed transform, which produce 4 scale segmentation results. The segmentation result marking with texture features in scale 2 is plotted in Figure 5. There are 104 regions in the result. It is shown that the region boundaries are congruent with most landscape objects. With the texture marking, the over-segmentation problem is solved so that the count of segments is decreased to a meaningful number. But it is also can be seen that there are some over-segmentation in severe texture areas and under-segmentation between different colour areas.

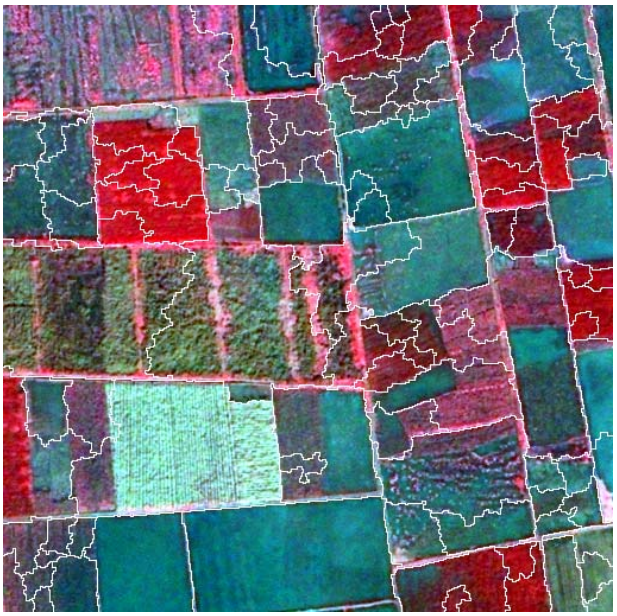

Figure 5. Segmentation result in scale 2

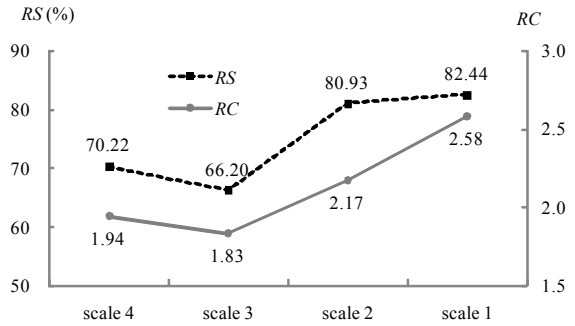

Figure 6. Segmentation accuracy in different scales

A reference map, as shown overlaid in Figure 1, is produced for quantitatively assess the segmentation accuracy in appropriate scale. The count of reference polygons is 48. The *RC* and *RS* of the segmentation results marking with different scale texture features is shown in Figure 6. Scale 1 is corresponding to the highest-frequency texture features, whereas scale 4 refers to the lowest ones. It can be seen that the region count parameter *RC* is increased with the texture marking from low frequency to high. That is, the segmentation will become more fragmental if

mark with more high-frequency texture. The fluctuated range of *RC* is 1.83 ~ 2.58, which is in an acceptable range.

As for the right segmented parameter *RS*, as shown in Figure 6, it is also increased with the texture marking from low frequency to high. The image is better segmented in small scale, that is, scale 1 and scale 2. Certainly, the region count is also more in these scales. *RS* of the image is between 66.2% ~ 82.44% for all of scales.

5. CONCLUSIONS

In conclusion, a scheme for segmenting high-spatial resolution satellite image based on vector field model and texture-marked watershed transform is proposed. With first fundamental form, the gradient information from all bands is accessed simultaneously, and the multiscale texture features of all bands are fused together. Moreover, the spectral information and texture information are integrated in the procedure of segmentation. The inclusion of texture features based on the actual frequency content of the image may ensure that differently textured regions are segmented effectively. Marking with different-frequency texture features may produce different scale segment-ation results, and the image is better segmented in small scale than large scale.

In experiments, the proposed method demonstrates excellent performance in very-high resolution image even where complicated agriculture areas. In particular, the proposed approach gives a better solution for the segmentation of multispectral remotely sensed image. It also has an effect of intrinsic hierarchy that reduces dramatically the over-segmentation problem of the watershed approach.

The drawback of the proposed method concerns the heavy computation of the multichannel log Gabor filtering, which may prevent the approach applied in real-time applications. Further study is needed on how to describe texture effectively even where the severe texture regions.

REFERENCES

Acharyya, M., De, R.K., Kundu, M.K., 2003. Segmentation of remotely sensed images using wavelet features and their evaluation in soft computing framework. *IEEE Transactions on Geoscience and Remote Sensing*, 41(12), pp. 2900-2905.

Baatz, M., Schape, A., 1999. Object-oriented and multi-scale image analysis in semantic networks. In: *Proceedings of the 2nd International Symposium on Operationalization of Remote Sensing*, ITC, Netherlands.

Blaschke, T., Lang, S., Lorup, E., Strobl, J., Zeil, P., 2000. Object-oriented image processing in an integrated GIS / remote sensing environment and perspectives for environmental applications. In: *Environmental Information for Planning, Politics and the Public*. Metropolis-Verlag, Marburg, Vol. 2, pp. 555-570.

Carleer, A.P., Debeir, O., Wolff, E., 2005. Assessment of very high spatial resolution satellite image segmentations. *Photogrammetric Engineering and Remote Sensing*, 71(11), pp. 1285-1294.

Chen, Z., Zhao, Z., Gong, P., Zeng, B., 2006. A new process for the segmentation of high resolution remote sensing imagery. *Inter-national Journal of Remote Sensing*, 27(22), pp. 4991-5001.

Cumani, A., 1991. Edge detection in multispectral images. *Computer Vision Graphics and Image Processing*, 53(1), pp. 40-51.

Devereuxa, B.J., Amablea, G.S., Posada, C.C., 2004. An efficient image segmentation algorithm for landscape analysis. *International Journal of Applied Earth Observation and Geoinformation*, 6, pp. 47-61.

Evans, C., Jones, R., Svalbe, I., Berman, M., 2002. Segmenting multispectral Landsat TM images into field units. *IEEE Transactions on Geoscience and Remote Sensing*. 40(5), pp. 1054-1064.

Field, D.J., 1987. Relations between the statistics of natural images and the response properties of cortical cells. *Journal of the Optical Society of America A*, 4(2), pp. 2379-2394.

Hall, O., Hay, G.J., Bouchard, A., Marceau, D.J., 2004. Detecting dominant landscape objects through multiple scales: an integration of object-specific methods and watershed segmentation. *Landscape Ecology*, 19(1), pp. 59-76.

Hill, P.R., Canagarajah, C.N., Bull, D.R., 2003. Image segmentation using a texture gradient based watershed transform. *IEEE Transactions on Image Processing*, 12(12), pp. 1618-1633.

Hu, X., Tao, C.V., Prenzel, B., 2005. Automatic segmentation of high-resolution satellite imagery by integrating texture, intensity, and color features. *Photogrammetric engineering and remote sensing*. 71(12), pp. 1399-1406.

Jain, A.K., Farrokhnia, F., 1991. Unsupervised texture segmentation using Gabor filters. *Pattern Recognition*, 24(12), pp. 1167-1186.

Kartikeyan, B., Sarkar, A., Majumder, K.L., 1998. A segmentation approach to classification of remote sensing imagery. *International Journal of Remote Sensing*, 19(9), pp. 1695-1709.

Kettig, R.L., Landgrebe, D.A., 1976. Classification of multispectral image data by extraction and classification of homogeneous objects. *IEEE Transactions on Geoscience Electronics*, GE-14(1), pp. 19-26.

Kovesi, P., 1996. *Invariant Measures of Image Features from Phase Information*. PhD dissertation, University of Western Australia, Nedlands, Western Australia, Australia.

Li, P., Xiao, X., 2007. Multispectral image segmentation by a multichannel watershed-based approach. *International Journal of Remote Sensing*, 28(19), pp. 4429-4452.

Li, W., Benie, G.B., He, D.C., Wang, S., Ziou, D., Hugh, Q., Gwyn, J., 1999. Watershed-based hierarchical SAR image segmentation. *International Journal of Remote Sensing*, 20(17), pp, 3377-3390.

Li, Y., Gong, P., 2005. An efficient texture image segmentation algorithm based on the GMRF model for classification of

remotely sensed imagery. *International Journal of Remote Sensing*, 26(22), pp. 5149-5159.

Lia, Y., Vodacek, A., Zhua, Y., 2007. An automatic statistical segmentation algorithm for extraction of fire and smoke regions. *Remote Sensing of Environment*, 108(2), pp. 171-178.

Pal, S.K., Ghosh, A., Shankar, B.U., 2000. Segmentation of Remotely Sensed Images with Fuzzy Thresholding, and Quantitative Evaluation. *International Journal of Remote Sensing*, 21(11), pp. 2269–2300.

Pekkarinen, A., 2002. A method for the segmentation of very high spatial resolution images of forested landscapes. *International Journal of Remote Sensing*, 23(14), pp. 2817-2836.

Pesaresi, M., Benediktsson, J.A., 2001. A new approach for the morphological segmentation of high-resolution satellite imagery. *IEEE Transactions on Geoscience and Remote Sensing*, 39(2), pp. 309-320.

Ryherd, S., Woodcock, C., 1996. Combining spectral and texture data in the segmentation of remotely sensed images. *Photogrammetric Engineering & Remote Sensing*, 62(2), pp. 181-194.

Sapiro, G., Ringach, D.L., 1996. Anisotropic Diffusion of Multivalued Images with Applications to Color Filtering. *IEEE Transactions on Image Processing*, 5(11), pp. 1582-1586.

Sarkar, A., Biswas, M.K., Kartikeyan, B., Kumar, V., Majumder, K.L., Pal, D.K., 2002. A MRF model-based segmentation approach to classification for multispectral imagery. *IEEE Transactions on Geoscience and Remote Sensing*, 40(5), pp. 1102-1113.

Scheunders, P., 2002. A multivalued image wavelet representation based on multiscale fundamental forms. *IEEE Transactions on Image Processing*, 10(5), pp. 568-575.

Scheunders, P., Backer, S.D., 2001. Fusion and merging of multispectral images with use of multiscale fundamental forms. *Journal of the Optical Society of America A*, 18(10), pp. 2468-2477.

Schiewe, J., 2002. Segmentation of high-resolution remotely sensed data – concepts, applications and problems. In: *International Archives of Photogrammetry, Remote Sensing and Spatial Information Sciences*, Ottawa, Canada, Vol. 34, pp. 380-385.

Vincent, L., Soille, P., 1991, Watershed in digital spaces: an efficient algorithm based on immersion simulations. *IEEE Transactions on Pattern Analysis and Machine Intelligence*, 13(6), pp. 583-598.

Wang, Z., Boesch, R., 2007. Color- and texture-based image segmentation for improved forest delineation. *IEEE Transactions on Geoscience and Remote Sensing*, 45(10), pp. 3055-3062.

Zenzo, S.D., 1986. A note on the Gradient of a Multi-image. *Computer Vision Graphics and Image Processing*, 33, pp. 116-125.

Zhang, Y., 2002. Problems in the fusion of commercial high-resolution satellite images as well as Landsat 7 images and initial solutions. In: *International Archives of Photogrammetry and Remote Sensing*, Ottawa, Canada, Vol. 34, Part 4, pp. 236-242.

Zhang, Y.J., 1996. A survey on evaluation methods for image segmentation. *Pattern Recognition*, 29(8), pp. 1335-1346.

ACKNOWLEDGMENTS

The research is supported by the National Natural Science Foundation of China with Grant No. 40771137 and 40501047.